European Journal of Medicinal Chemistry 47 (2012) 601–607

Contents lists available at SciVerse ScienceDirect

European Journal of Medicinal Chemistry

journal homepage: http://www.elsevier.com/locate/ejmech

Short communication

A novel caryophyllene type sesquiterpene lactone from *Asparagus falcatus* (Linn.); Structure elucidation and anti-angiogenic activity on HUVECs

Raza Murad Ghalib [a,*], Rokiah Hashim [b], Othman Sulaiman [a], Sayed Hasan Mehdi [a], Arto Valkonen [b,1], Kari Rissanen [b,1], Srećko R. Trifunović [c], Mohamed. B. Khadeer Ahamed [d], Amin Malik Shah Abdul Majid [d], Fumio Kawamura [e]

[a] School of Industrial Technology, Universiti Sains Malaysia, 11800 Minden, Pulau Pinang, Malaysia
[b] Nanoscience Center, Department of Chemistry, P.O. Box 35, 40014, University of Jyväskylä, Finland
[c] Department of Chemistry, Faculty of Science, University of Kragujevac, 34000 Kragujevac, Serbia
[d] Department of Pharmacology, School of Pharmaceutical Sciences, Universiti Sains Malaysia, 11800 Minden, Pulau Pinang, Malaysia
[e] Wood Extractives Laboratory, Department of Biomass Chemistry, Forestry and Forest Products Research Institute (FFPRI), Tsukuba 305-8687, Japan

ARTICLE INFO

Article history:
Received 22 April 2011
Received in revised form
7 October 2011
Accepted 18 October 2011
Available online 25 October 2011

Keywords:
Asparagus falcatus (Linn.)
Aspfalcolide
Crystal structure
Anti-angiogenic activity
HUVECs

ABSTRACT

In this study the novel caryophyllene type sesquiterpene lactone (aspfalcolide) has been isolated from the leaves of *Asparagus falcatus* (Linn.) and characterized by IR, 1D NMR, 2D NMR, EI–MS, HR–ESI–MS and X-ray single crystal diffraction analysis. The aspfalcolide crystallizes in the orthorhombic space group $P2_12_12_1$ with $a = 6.37360(10)$, $b = 7.6890(2)$, $c = 27.3281(6)$ Å, $\alpha = \beta = \gamma = 90^{\circ}$ and $Z = 4$. One intermolecular O–H···O hydrogen bond enforces these natural molecules to form infinite chains through the crystal. Aspfalcolide was screened for its anti-angiogenic activity in human umbilical vein endothelial cells (HUVECs) and the result showed the remarkable inhibitory effect of aspfalcolide on the proliferation (IC_{50} 1.82 μM), migration and tube formation of HUVECs.

1. Introduction

Asparagus falcatus (Linn.) is a traditional medicinal scandent shrub which belongs to the family of Asparagaceae. The plant is distributed abundantly in South Africa, Swaziland, Mozambique and some parts of East Asia. The stems and leaves are pounded and used as a fresh poultice on swellings. This plant has been used in traditional Chinese medicine for over 2000 years for the treatment of cancer. The plant has dynamic pharmacological properties such as antibacterial, anti-inflammatory, antipyretic, antiseptic, antitussive, diuretic, expectorant, nervine, sialagogue, stomachic, nervous stimulant and tonic. It is taken internally in the treatment of fevers, debility, sore throats and coughs [1–3].

The effect of *A. falcatus* extract on acetaminophen-induced liver injury was investigated *in vivo* and the results suggest that the feeding regimen with Asparagus extract inhibited the progression of hepatic injury induced by acetaminophen [4]. Previously phytoecdysteroids [5] as well as capsoneoxanthin [6] and (9*Z*)-Capsanthin-5,6-epoxide [7] carotenoids have been reported from the ripe fruits of *A. falcatus*. In an investigation on carotenoids present in the fruit of *A. falcatus*, capsanthin, capsorubin, 5,6-diepikarpoxanthin, capsanthin-5,6-epoxide, capsochrome, mutatoxanthin, antheraxanthin, and capsanthone have been isolated [8]. *A. falcatus* is also a natural source of steroid sapogenins, as sarsasapogenin from its root [9]. 3,5,4′-Trihydroxy-6,7-dimethoxyflavone (eupalitin) has recently been reported from this plant [10].

Caryophyllene type sesquiterpene lactone has been discovered from the plant *A. falcatus* for the first time, though the Asparagaceae family is enriched with terpenes. Plant products rich in sesquiterpene lactones have been used in traditional medicines [11]. Several studies showed that sesquiterpene lactones posses strong inflammatory, anti-tumor and antimicrobial activities [12–14]. Since then, this class of phytochemicals has attracted the attention of researchers towards their potential medicinal properties. Several sesquiterpene lactones such as artemisinins, thapsigargins, parthenolide etc., have demonstrated the ability to inhibit the angiogenesis *in vitro* as well as *in vivo* by inhibiting HUVEC

* Corresponding author. Tel.: +60 164526657; fax: +60 4 6573678.
E-mail address: raza2005communications@gmail.com (R.M. Ghalib).
[1] X-ray crystallography.

0223-5234/$ – see front matter © 2011 Elsevier Masson SAS. All rights reserved.
doi:10.1016/j.ejmech.2011.10.037

proliferation, microvessel formation and proliferation of human artery endothelial cells, and by suppressing vascular endothelial growth factor (VEGF) and receptor expression and osteolytic bone metastasis [15–17]. Biological activities can be affected by three major chemical properties of sesquiterpene lactones, which comprise alkylating center reactivity, lipophilicity, and electronic features. Hartwell and Abbott [18] reported that the α-methylene-γ-lactone moiety of sesquiterpene lactones has direct influence on their biological activity. This α-methylene-γ-lactone moiety reacted via Michael-type addition with biological nucleophiles such as the thiol group containing cysteine residues in proteins, which helps in formation of the stable adducts [19]. Additionally, the unsaturated carbonyl or '-enone' (O═C–C═CH_2) system in lactones enhances the biological activity of sesquiterpene lactones [20,21]. Several studies proved that sesquiterpene lactones have an ability to bind to blood proteins containing sulfhydryl groups [22], and also form glutathione adducts by interacting with red blood cells, which are known to contain high glutathione content [23].

The second property of sesquiterpene lactones is their lipophilicity. Generally, higher lipophilicity facilitates the compound in penetration through the cell membrane, thereby increasing sesquiterpene lactones bioavailability *in vitro*. The addition of a lipophilic moiety showed elevated anti-cancer activity against Ehrlich ascites carcinoma *in vitro* and *in vivo* [20]. Another well-known property attributed to the structure–bioactivity relationship in sesquiterpene lactones is the contribution of oxygen atoms and atomic charges present in the molecular surface areas [24]. Altogether, these above mentioned favorable features make sesquiterpene lactones promising candidates in the drug discovery research. In this paper we reported the isolation and structure determination of novel sesquiterpene lactone (aspfalcolide) (Fig. 1A and B) from the leaves of *A. falcatus*. Furthermore, we assessed the possible anti-angiogenic activity of the isolated compound on the proliferation, migration and tube formation of HUVECs.

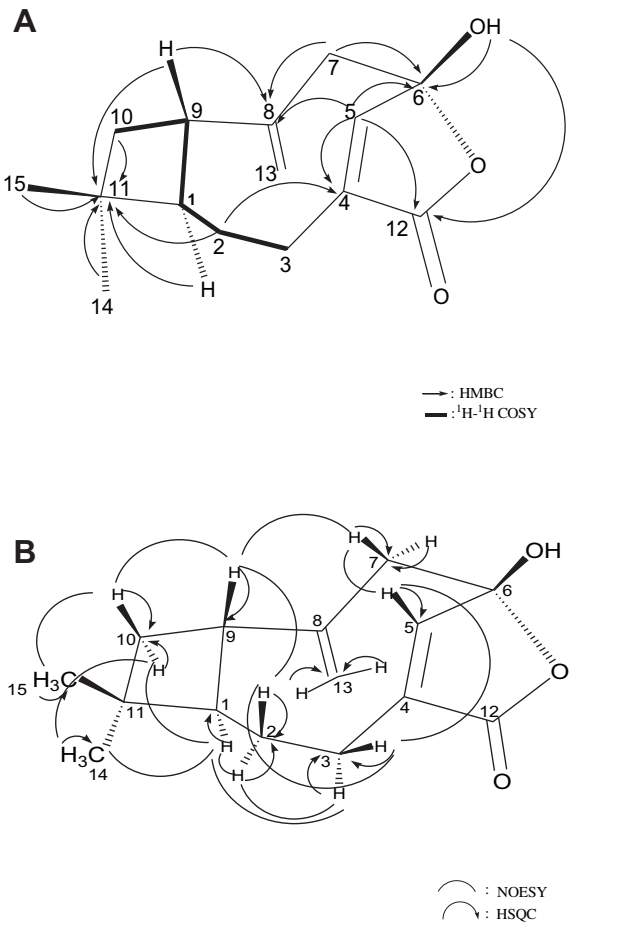

Fig. 1. A. The ^{1}H–^{1}H COSY and selective HMBC correlations of aspfalcolide, B. HSQC and selective NOESY correlations of aspfalcolide.

2. Results and discussion

2.1. Chemistry

The compound was obtained as transparent crystals. The molecular formula was determined as $C_{15}H_{20}O_3$ (six degrees of unsaturation) by analysis of ^{13}C and ^{1}H NMR data in conjugation with DEPT results (Table 1), and this conclusion was further confirmed by EI–MS and HR–ESI–MS. The ^{13}C NMR spectrum displayed 15 carbons, which were assigned by HSQC, HMBC and DEPT experiments to the resonances of 2 CH_3, 5 CH_2, 3 CH and 5 Cs. In the ^{1}H NMR and ^{13}C NMR spectra of the compound, one proton signal δ 6.84 (1H, *d*, H-5) and four carbon signals [δ 171.61 (C-12), 136.01 (C-4), 105.43 (C-6), 147.08 (C-5)], were observed which suggests the presence of γ-hydroxy-α,β-unsaturated γ-lactone with additional substitution at β and γ positions. The presence of an α,β-unsaturated γ-lactone was further supported by the strong absorption at 1705 cm^{-1} which must be at 1760 cm^{-1}, but due to the presence of strong intermolecular O–H···O═C hydrogen bonding (Fig. 3), the IR value decreases. The third oxygen atom is present as an OH group as indicated by the broad band at 3392 cm^{-1} in IR spectrum and a broad singlet at δ 4.05 in ^{1}H NMR spectrum. Detailed 2D NMR analysis showed that compound is a caryophyllene type sesquiterpene lactone which is composed of cyclobutane, cyclononene and 2(*5H*)-furanone cyclic systems. From the ^{1}H–^{1}H COSY spectrum of aspfalcolide (Fig. 1A), it was possible to establish the spin systems that enabled identification of the H-1/H_2-2, H_2-2/H_2-3, H-9/H_2-10 and H-1/H-9 (C-3/C-2/C-1, C-9/C-10 and C-1/C-9 units). Based on these data, together with HMBC correlations between H-1/C-2, C-9, C-8; H_2-2/C-4, C-3, C-1, C-9, C-5; H_2-3/C-2; H-5/C-3, C-4, C-6, C-7, C-8; H-$_2$-7/C-9, C-8, C-6, C-5; H-9/C-1, C-8 established a connectivity to form the nine member ring (C1–C2–C3–C4–C5–C6–C7–C8–C9).

Table 1
Spectroscopic data for aspfalcolide.

Position	^{13}C	DEPT	^{1}H	HMBC (H→C)
1	56.32	CH	1.50 m	2, 8,9,11,15
2α	29.64	CH_2	1.55 m	1, 3, 4, 5, 9, 11, 14, 15
β			1.70 m	10
3α	21.86	CH_2	2.30 m	2
β			2.44 m	–
4	136.01	C	–	–
5	147.08	CH	6.84 d (2.0)	3, 4, 6, 7, 8, 12
6	105.43	C	–	–
7α	49.80	CH_2	2.87 d (12.8)	5, 6, 8, 9, 10, 13
β			2.50 d (12.8)	6, 8, 9, 10, 13
8	146.27	C	–	–
9	46.85	CH	2.03 m	1, 8,10, 11
10α	43.83	CH_2	1.58 dd (10.8, 6.2)	–
β			1.87 dd (10.8, 8.0)	1, 11, 15
11	32.76	C	–	–
12	171.61	C	–	–
13	120.44	CH_2	5.18 s	1, 7, 9, 10
			5.28 s	1, 7, 9, 10
14	29.53	CH_3	0.99 s	1, 2, 10,11, 15
15	22.09	CH_3	0.98 s	1, 2, 10, 11, 14
OH	–	–	4.05 s	5,6,7, 12

Coupling constants (Hz) in parentheses.
–: Not detected.

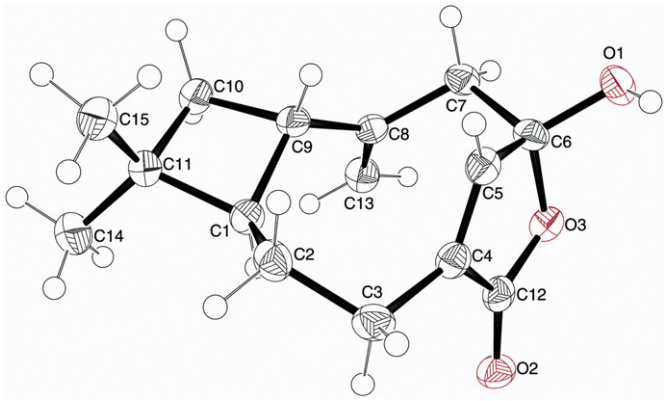

Fig. 2. ORTEP plot and atom numbering of aspfalcolide.

Table 2
Selected bond lengths [Å] and angles [°] for aspfalcolide.

O(1)–C(6)	1.383(3)	C(10)–C(11)–C(1)	88.6(2)
O(3)–C(12)	1.338(3)	C(11)–C(10)–C(9)	89.8(2)
O(3)–C(6)	1.471(3)	C(10)–C(9)–C(1)	88.11(19)
O(2)–C(12)	1.221(4)		
C(4)–C(5)	1.324(4)	C(9)–C(1)–C(11)–C(10)	17.3(2)
C(4)–C(12)	1.481(4)	C(1)–C(11)–C(10)–C(9)	−17.5(2)
C(3)–C(4)	1.499(4)	C(11)–C(10)–C(9)–C(1)	17.5(2)
C(8)–C(13)	1.318(4)	C(11)–C(1)–C(9)–C(10)	−17.2(2)
C(5)–C(6)	1.496(4)	C(12)–O(3)–C(6)–C(5)	12.1(3)
		O(3)–C(6)–C(5)–C(4)	−14.6(3)
C(12)–O(3)–C(6)	108.3(2)	C(5)–C(4)–C(12)–O(3)	−3.4(3)
C(5)–C(4)–C(12)	107.0(2)	C(6)–O(3)–C(12)–C(4)	−6.1(3)
C(11)–C(1)–C(9)	88.1(2)	C(6)–O(3)–C(12)–O(2)	176.0(2)

Furthermore key HMBC correlations between H_2-2/C-11; H-1/C-11; H-9/C-1, C-10, C-11; H-10/C-1, C-11 established cyclobutane ring (C-1-C-11-C-10-C-9) fused to nine membered ring at C-1 and C-9. The geminal location of both the C-15 (δ 22.09) and C-14 (δ 29.53) methyl carbons on C-11 was deduced from ^3J-HMBC correlation to each other and ^2J-HMBC correlation to the same quaternary carbon (C-11, δ 32.76) (Table 1). The presence of an exomethylene group was supported by two one proton singlets (δ 5.18 and δ 5.28) and two carbon signals (δ 146.27 and δ 120.44) in ^{1}H and ^{13}C spectra. The $\Delta^{8,13}$ system was assigned on the basis of the ^3J-HMBC correlation between H_2-13/C-9, C-7. The hydroxyl group (δ 4.05) positioned at C-6 (δ 105.43) was confirmed by the connectivity between OH/C-7, C-6, C-5. The key HMBC correlations between H-5/C-12 and OH/C-12 suggest the five-membered lactone ring system fused at C-4, C-5 and C-6.

The relative stereochemistry of three stereo centers C-1, C-6 and C-9 were established as (1R*, 6R*, 9S*) from the NOE interactions observed in the NOESY spectrum (Fig. 1B). Based on above data aspfalcolide was elucidated to be as (+)-(1R*, 6R*, 9S*)-6-hydroxy-11,11-dimethyl-8-methylene-bicyclo[7.2.0]-undec-4(5)-en-6(4)-olide (Fig. 1B).

2.2. Crystal structure determination of aspfalcolide

The crystal structure of the molecular unit of the aspfalcolide with the atomic numbering scheme used is shown in Fig. 2. The absolute configuration of it remained unknown after the single crystal x-ray analysis with CuK_α-radiation, due to poor anomalous scattering effects of the compound. The meaningless absolute structure parameter value ~0.40 [25] was removed from the data. Refinements by twinned crystal methods were not successful, indicating that the crystal is not racemic or (non)merohedral twin. The selected bond lengths and angles for the isolated compound are listed in Table 2. Packing diagram with classical O–H···O hydrogen bonds in the crystal are shown in Fig. 3. This compound is composed of three condensed cyclic systems: cyclobutane (C1–C9–C10–C11), cyclononene (C1–C2–C3–C4–C5–C6–C7–C8–C9) and 2(*5H*)-furanone (C4–C5–C6–O3–C12). The angles between carbon atoms in cyclobutane ring are between 88 and 90° (Table 2). All torsion angles are close to +17 or −17°. One carbon is out of plane of the rest three carbons making "*puckered*" conformation of the cyclobutane ring (Fig. 2). For example, atom C11 makes a ~24.5° angle with the plane formed by C1, C9 and C10, a slightly smaller than in free cyclobutane [26].

The 2(*5H*)-furanone ring is on the opposite side of the molecule from cyclobutane ring and the whole tricyclo system forms *chair*-like conformation (Figs. 2 and 3). The C6 atom is out of C4–C5–O3–C12 plane [with torsion angles of 12.1(3)° for C12–O3–C6–C5 and −14.6(3)° for O3–C6–C5–C4] forming a ~13.3° angle to the plane and a conformation intermediate between *planar* and *envelope* for 2(*5H*)-furanone ring (Fig. 3, Table 2). The short C4–C5 and C12–O2 bond lengths (Table 3) prove the double C–C and C–O bonds, respectively. The bonds O3–C12 and O3–C6 in this lactone are different, due to the slight double bond character of the former, suggesting the deformation of this five-membered ring although there are no significant differences in angles in the ring (Table 2). In the flexible central cyclononene ring, there are only one double C4–C5 bond in the ring and one, C8–C13, out of the ring. Both of them are almost of the same length (Table 2) and the ring forms specific conformation (Figs. 2 and 3). All the rest bond lengths and angles in the tricyclo system are in expected range for single C–C bonds and tetrahedral

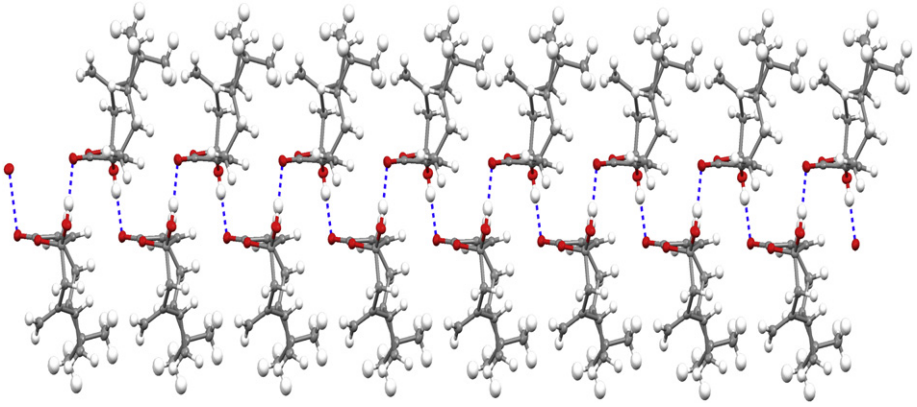

Fig. 3. Infinite chain along the *a* axes in crystal structure of aspfalcolide. Double-dotted lines represent hydrogen bonds.

Table 3
Selected intermolecular short contacts [Å, °] in aspfalcolide.

D–H···A	d(D···A)/Å	<(DHA)/°
O(1)–H(1O)···O(2)[a]	2.800(3)	169(4)
C(13)–H(13B)···O(1)[b]	3.423(4)	160(4)

Symmetry transformations used to generate equivalent atoms:
[a] x+1/2, −y+1/2, −z.
[b] x−1/2, −y+3/2, −z.

arrangement around carbon atoms. The presence of one –OH group in molecular structure (Fig. 1) indicates that the hydrogen bonds should be present in the crystal and they would take a very significant role in a packing way. The presence of strong intermolecular O1–H1O···O2 hydrogen bonds was confirmed (Table 3) and they were found to connect the molecules as infinite chains along the *a* axis (Figs. 3 and 4). These chains are connected to each other by weak C–H···O interactions between methylidene protons at C13 and O1 (Table 3).

3. Pharmacology

3.1. Inhibition of VEGF-Induced HUVECs proliferation

In order to evaluate the effect of aspfalcolide on human umbilical vein endothelial cells (HUVECs), an investigation on a series of angiogenesis related aspects of endothelial cells were conducted. We first determined whether aspfalcolide inhibited the VEGF-induced endothelial cell proliferation. The result showed a dose-dependent inhibition of the endothelial cell proliferation after 48 h by aspfalcolide (Fig. 5). The compound showed significant inhibition with IC_{50} 1.82 μM but it failed to show complete inhibition even at higher concentration (3.2 μM), whereas the reference standard, suramin exhibited almost complete inhibition of proliferation with IC_{50} 0.52 μM.

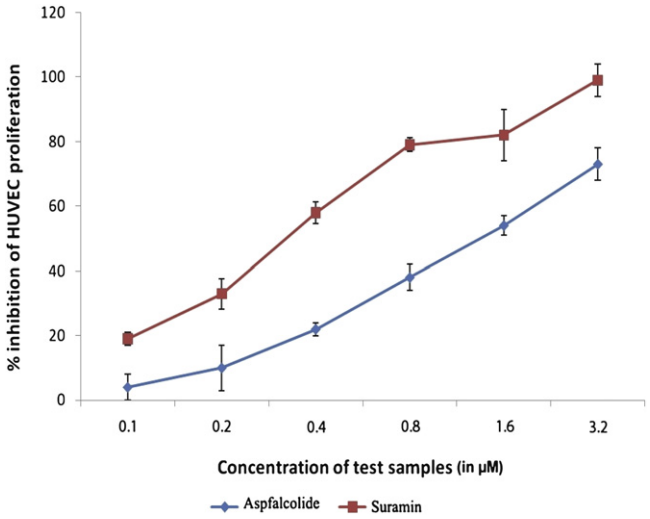

Fig. 5. The dose-dependent inhibitory effects of aspfalcolide and suramin on VEGF-induced proliferation of endothelial cells. Data is presented in Mean ± S.E. ($n = 3$).

3.2. Inhibitory effect of aspfalcolide on HUVECs migration

To evaluate the inhibitory effect of aspfalcolide on endothelial cell migration process, *in vitro* wound healing assay was conducted. This assay represents an important step in the formation of new blood vessels and is a straightforward and economical method to study the cell migration phenomenon [27]. A scratch wound was created on the monolayer of cells. Aspfalcolide (1.6 μM) inhibited HUVECs migration drastically by 18.5% after 12 h and 21.9% after 18 h ($P < 0.001$), whereas, the reference standard, suramin (0.5 μM) inhibited the migration of endothelial cells completely (Fig. 6).

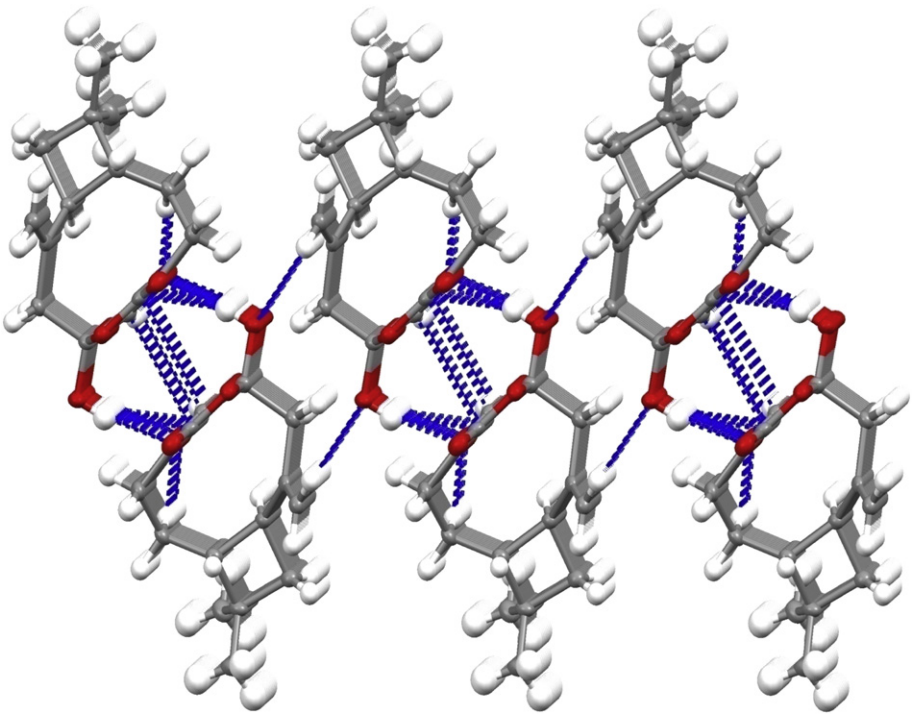

Fig. 4. A view along the *a* axes. Double-dotted lines represent hydrogen bonds.

3.3. Inhibitory effect of aspfalcolide on tube formation in HUVECs

To determine the effect of aspfalcolide on tube formation property of HUVECs, endothelial cells tube formation assay was carried out. Aspfalcolide inhibited the growth factor induced tube formation of endothelial cells on Matrigel. Fig. 7 depicted the inhibitory effect of aspfalcolide on tube formation by HUVECs. Endothelial cells formed tube-like networks (Fig. 7A) within 6 h, which might, in part, reflect the process of angiogenesis. At a concentration of 1.6 μM (Fig. 7B), aspfalcolide significantly inhibited the tube formation by reducing the tube-like structure both in width and in length. Whereas, endothelial cells rounded up and rendered network structures incomplete and broken in the presence of suramin (Fig. 7C).

4. Experimental

4.1. Physical measurements

Optical rotation was determined on a JASCO DIP-140 polarimeter. The melting point was taken on Thermo Fisher digital melting point apparatus of IA9000 series. IR spectrum was taken on Shimadzu IR-408 Perkin Elmer 1800 (FTIR). ^{1}H NMR was recorded on Bruker Avance 400 MHz with TMS as an internal standard and 100 MHz for ^{13}C NMR. Spectra were recorded in $CDCl_3$. EI–MS was recorded on JEOL GCmate instrument in ionization mode. HR-ESI-MS was recorded on a Finnigan TSQ Quantum Ultra AM Thermo Electron. Open column chromatography was performed on silica gel 60 (Merck, 0.04–0.063 mm, 230–400 mesh ASTM) and Sephadex LH-20 (Pharmacia). TLCs were taken on silica gel plates (silica gel 60 F_{254} on aluminum foil, Merck).

4.2. Plant material

The leaves of *A. falcatus* were collected from the South Africa and identified by Mrs. Siti Nurdijati Baharuddin Taxonomist and lecturer, School of Biological sciences, USM, Malaysia. A sample voucher specimen of the plant has been submitted at herbarium in the School of Biological sciences, USM, Malaysia under voucher specimen No. 11129.

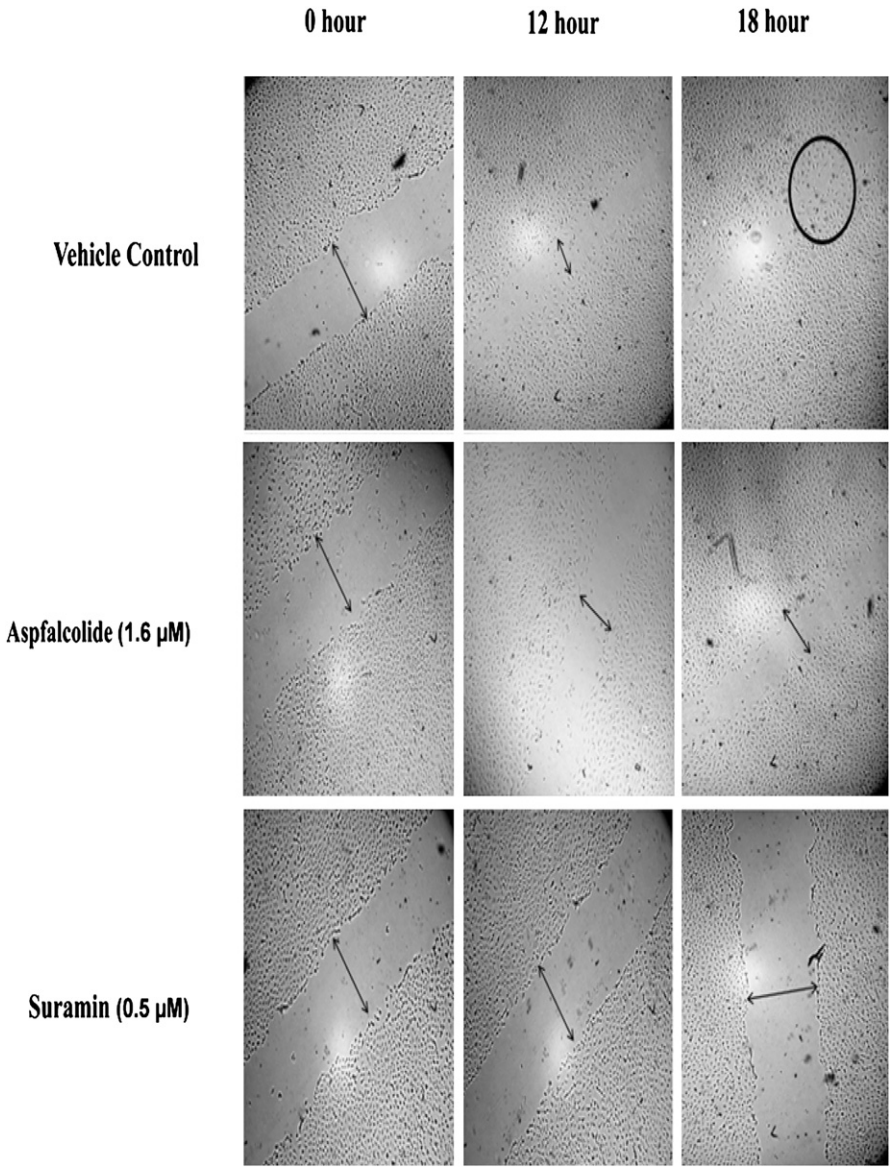

Fig. 6. Inhibitory effect of aspfalcolide on migration of endothelial cells. Data is presented in Mean ± S.E. ($n = 3$).

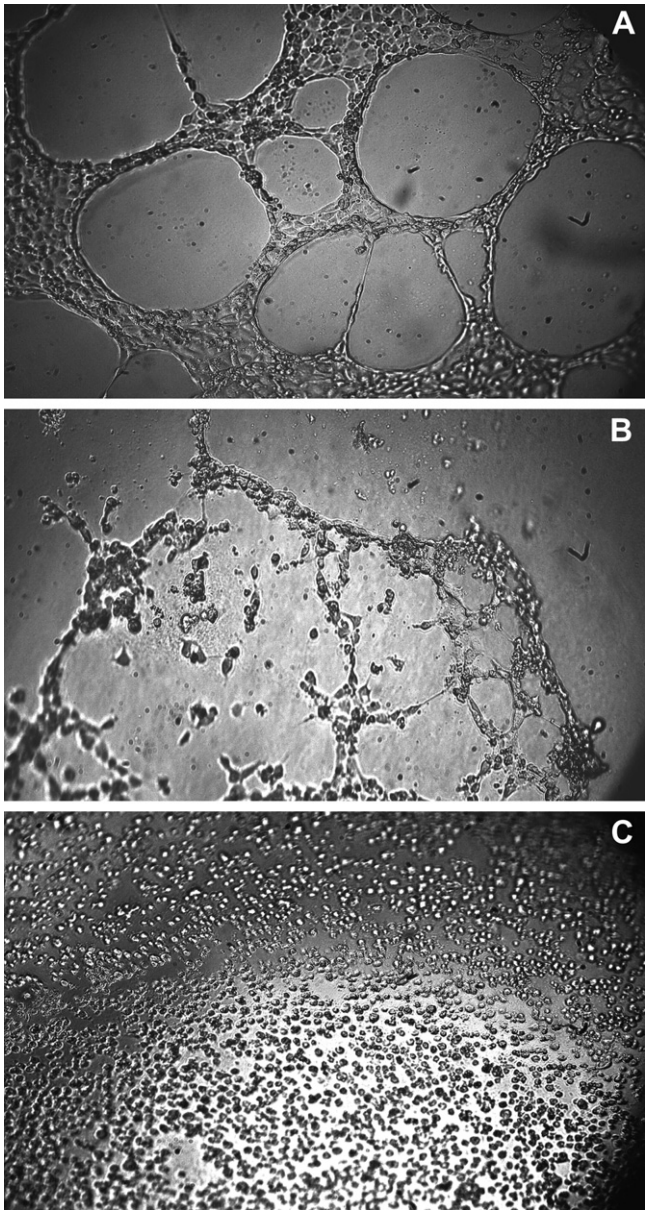

Fig. 7. Anti-angiogenesis ability of aspfalcolide by inhibiting the tube formation in HUVECs. Growth factors-induced endothelial cells formed tube-like networks, A. within 6 h after the seeding, which might, in part, reflect the initiation process of angiogenesis. At a concentration of 1.6 μM, B. The aspfalcolide significantly inhibited the endothelial tube formation by reducing the tube-like structure both in width and in length. The standard drug suramin absolutely abrogated the tube-like structure in endothelial cells at a concentration of 0.5 μM, C. Data is presented in Mean ± S.E. ($n = 3$).

4.3. Extraction and isolation

The air dried and crushed leaves (1.0 kg) of the plant species were thoroughly extracted with chloroform. The extract was concentrated in rotary evaporator at low pressure and then it was chromatographed using a silica gel column loaded with petroleum ether, eluted with a stepwise gradient of light petroleum ether, light petroleum ether/diethylether (9:1–1:1), ethyl acetate and ethyl acetate/methanol (9:1–1:1). The elutants obtained through petroleum ether/diethylether solvent system (9:1–7:3) yielded aspfalcolide (500 mg, mp. 191.4 °C). This was further purified through recrystallization with the aid of chloroform/dry alcohol (1:1 *v*/*v*) to afford the transparent crystals.

4.4. Aspfalcholide

Transparent crystalline solid (500 mg) (mp. 191.4 °C); $[\alpha]_D^{20}$ + 7.03 (*c* 1.14, $CHCl_3$); IR (KBr) ν_{max} 3392, 3089, 3067, 2988, 3939, 2879, 2854, 1705, 1647, 1453, 1438, 1402, 1336, 1123, 1062, 962, 960, 914, 868, 766, 739, 728, 669 cm^{-1}; EIMS *m*/*z* 249.1955 $[M + H]^+$ (2.5%), *m*/*z* 248.1711 $[M]^+$(12.1%); HR–ESI–MS m/z 249.1416 (small peak) $[M + H]^+$ Calc. *m*/*z* 249.1491$[M + H]^+$ for $C_{15}H_{21}O_3$ Composition: C 72.6%, H 8.1%, O 19.3%; *m*/*z* 271.1102 $[M + Na]^+$ calc. 271.1310 $[M + Na]^+$ for $C_{15}H_{20}O_3Na$; *m*/*z* 303.1261 $[M + Na + CH_3OH]^+$ calc. 303.1572 $[M + Na + CH_3OH]^+$for $C_{16}H_{24}O_4Na$; ^1H NMR (400 MHz, CDCl3); ^{13}C NMR (100 MHz, $CDCl_3$) (see Table 1)

4.5. Single crystal analysis

The structural data were collected at 123 ± 2 K with a Bruker–Nonius KappaCCD diffractometer equipped with APEXII detector using graphite monochromatised CuK_α radiation ($\lambda = 1.54184$ Å). The COLLECT [28] data collection software was used and obtained data were processed with DENZO-SMN [29]. The structures were solved by direct methods, using SIR-2004 [30] and refined on F^2, using SHELXL-97 [31]. The reflections were corrected for Lorenz polarization effects and multi-scan absorption correction [32] was applied on the data. The hydrogen atoms (except –OH) were calculated to their idealized positions with isotropic temperature factors (1.2 or 1.5 times the C temperature factor) and refined as riding atoms. Hydrogen atom of –OH group was found from the electron density maps and fixed to a distance of 0.84 Å from O atom with isotropic temperature factor (1.5 times the O temperature factor). The figures were drawn with ORTEP-3 [33] and MERCURY [34]. Other experimental X-ray data are shown in Table 4.

4.6. HUVEC proliferation assay

HUVECs were maintained in ECM containing 5% HIFBS and 1% PS, 1% ECGS. The cells were seeded in 96-well plates at a density of 2 × 104 cells/well in 100 μl growth media and kept overnight to facilitate attachment. The cells were exposed to the test samples (0.01–3.2 μM) for 48 h [35]. After incubation, the viability of HUVECs was assessed by MTT (3-(4,5-dimethylthiazol-2-yl)-2,5-diphenyltetrazolim bromide) assay [36]. 20 μl of MTT solution (5 mg/mL in PBS) was added to each well. After 4 h incubation, the mixed media and MTT solution were carefully discarded and then

Table 4
Crystal data and structure refinement for aspfalcolide.

Formula	$C_{15}H_{20}O_3$
M/g mol^{-1}	248.31
System	Orthorhombic
Space group/*Z*	$P2_12_12_1/4$
a/Å	6.3724(5)
b/Å	7.6888(6)
c/Å	27.309(2)
α,*β*,*γ*/°	90
V/$Å^3$	1338.0(2)
D/g cm^{-3}	1.233
F(000)	536
μ/cm^{-1}	0.680
θ(min–max)/°	5.98–63.32
Collected reflections	5222
Unique reflections [$I > 2\sigma(I)$]	1269
R_{int}	0.0585
R/w*R*2 [$I > 2\sigma(I)$]	0.0424/0.1127
R/w*R*2 (All)	0.0455/0.1151
Largest diffr. peak and hole/e $Å^{-3}$	0.190 and −0.204

the crystallized dye was solubilized with DMSO. Suramin was used as the reference standard. The amount of blue dye formed was determined by measuring the absorbance at 570 nm.

4.7. Migration assay

The assay was carried out according to Liang et al. [27], with minor modifications. Briefly, HUVECs were plated in 6 well plates. After the formation of a confluent monolayer, a wound was created using 200 μl micropipette tip. The free cells were removed by washing twice with PBS. Aspfalcolide (1.6 μM) and suramin (0.5 μM) were added to the separate wells containing cells within a fresh media containing 10% calf serum. After 12 and 18 h, the wounds were photographed and distances between one side of the scratch and the other were measured using inverted light microscope supplied with Leica Quin computerized imaging system. 10 fields for each concentration were captured and minimum 10 readings of distance for each field were measured.

4.8. VEGF-induced tube formation assay

HUVECs were harvested and seeded in ECM medium (5% HIFBS) containing VEGF (100 ng/mL) onto 4-well culture plates coated with 150 μl Matrigel (5 mg/mL). The cells were treated with aspfalcolide (1.6 μM) and incubated at 37 °C for 24 h. Suramin was used as a positive control at 0.5 μM in the growth medium. The cells were imaged under an inverted florescence microscope at low magnification. The web junctions, defined as intersections of three or more tubes, were counted in each microscopic field [37]. The quantitative assessment of tube formation inhibition was achieved by measuring the area of formed tubes in each field using the Scion Image analysis program. The percentage of inhibition was represented as the mean ± SEM.

Acknowledgments

We would like to acknowledge Universiti Sains Malaysia (USM) for the University Grant 1001/PTEKIND/8140152. The authors are grateful to the Ministry of Science and Technological Development of the Republic Serbia for financial support (Project No 172016). We also gratefully acknowledge the Academy of Finland (proj. no. 212588) and the University of Jyväskylä for funding.

Appendix. Supplementary data

CCDC-757069 contains the supplementary crystallographic data for this structure determination. These data can be obtained free of charge via http://www.ccdc.cam.ac.uk/conts/retrieving.html (or from the Cambridge Crystallographic Data Centre, 12, Union Road, Cambridge CB2 1EZ, UK; fax: +44 1223 336033).

References

[1] J.A. Duke, E.S. Ayensu, Medicinal Plants of China. Reference Publications, Inc, 1985, ISBN 0-917256-20-4.
[2] H. Yeung, Handbook of Chinese Herbs and Formulas. Institute of Chinese Medicine, Los Angeles, 1985.
[3] V.D. Nguyen, T.N. Doan, Medicinal Plants in Vietnam. World Health Organisation, 1989, ISBN 92 9061 101 4.
[4] R.P. Hewawasam, K.A.P.W. Jayatilaka, C. Pathirana, J. Diet. (2008) 1–19 Suppl. 5.
[5] L. Dinan, T. Savchenko, P. Whiting, Phytochemistry 56 (2001) 569–576.
[6] J. Deli, P. Molnár, E. Osz, G. Tóth, Tetrahedron Lett. 41 (2000) 8153–8155.
[7] P. Molnár, J. Deli, G. Tóth, A. Häberli, H. Pfander, K. Bernhard, J. Nat. Prod. 64 (2001) 1254–1255.
[8] J. Deli, P. Molnár, E. Osz, G. Tóth, Chromatographia 51 (2000) S183–S187.
[9] F.D. Ricardo, F.R. Barreira, G.G. Antonio, Quimica 63 (1967) 939–944.
[10] R.M. Ghalib, S.H. Mehdi, R. Hashim, O. Sulaiman, A. Valkonen, K. Rissanen, S.R. Trifunović, J. Chem. Cryst. 6 (2010) 510–513.
[11] D.S. Seigler, Plant Secondary Metabolism. Kluwer Academic, Norwell, MA, 1998, 367–398.
[12] E. Koch, C.A. Klaas, P. Rüngeler, V. Castro, G. Mora, W. Vichnewski, I. Merfort, Biochem. Pharmacol. 62 (2001) 795–801.
[13] J.Q. Gu, J.J. Gills, E.J. Park, E. Mata-Greenwood, M.E. Hawthorne, F. Axelrod, P.I. Chavez, H.H.S. Fong, R.G. Mehta, J.M. Pezzuto, A.D. Kinghorn, J. Nat. Prod. 65 (2002) 532–536.
[14] C.A. Obafemi, T.O. Sulaimon, D.A. Akinpelu, T.A. Olugbade, Afr. J. Biotech. 5 (2006) 1254–1258.
[15] H.H. Chen, H.J. Zhou, G.D. Wu, X.E. Lou, Pharmacol 71 (2004) 1–9.
[16] N. Shukla, N. Freeman, P. Gadsdon, G.D. Angelini, J.Y. Jeremy, Cardiovasc. Res. 49 (2001) 681–689.
[17] A.I. Idris, H. Libouban, H. Nyangoga, E. Landao-Bassonga, D. Chappard, S.H. Ralston, Mol. Cancer Ther. 8 (2009) 2339–2347.
[18] J.L. Hartwell, B.J. Abbott, Antineoplastic principles in plants: recent developments in the field, Adv. Pharmacol. Chemother. 7 (1969) 117–120.
[19] S.M. Kupchan, D.C. Fessler, M.A. Eakin, T.J. Giacobbe, Science 168 (1970) 376–378.
[20] K.H. Lee, R. Meck, C. Piantadosi, E.S. Huang, J. Med. Chem. 16 (1973) 299–301.
[21] K.H. Lee, I.H. Hall, E.C. Mar, C.O. Starnes, S.A. ElGebaly, T.G. Waddell, R.I. Hadgraft, C.G. Ruffner, I. Weidner, Science 196 (1977) 533–536.
[22] S. Wagner, Planta Med. 70 (2004) 227–233.
[23] T.J. Schmidt, G. Lyss, H.L. Pahl, I. Merfort, Bioorg. Med. Chem. 7 (1999) 2849–2855.
[24] T.J. Schmidt, J. Heilmann, Quant. Struct. Act. Relat. 21 (2002) 276–287.
[25] H.D. Flack, Acta Cryst. A39 (1983) 876–881.
[26] E.D. Glendening, A.M. Halpern, J. Phys. Chem. 109 (2005) 635–642.
[27] C.C. Liang, A.Y. Park, J.L. Guan, Nat. Protoc. 2 (2007) 329–333.
[28] Bruker, COLLECT Data Collection Software, 2008. Bruker AXS, Delft, The Netherlands, 2008.
[29] Z. Otwinowski, W. Minor, Processing of X-ray diffraction data collected in oscillation mode. in: C.W. Carter Jr., R.M. Sweet (Eds.), Methods in Enzymology, Macromolecular Crystallography, Part A, 276. Academic Press, New York, 1997, pp. 307–326.
[30] M.C. Burla, R. Caliandro, M. Camalli, B. Carrozzini, G. Cascarano, C. Giacovazzo, G. Polidori, R. Spagna, J. Appl. Cryst. 38 (2005) 381–388.
[31] G.M. Sheldrick, Acta Cryst. A64 (2008) 112–122.
[32] G.M. Sheldrick, SADABS. University of Göttingen, Göttingen Germany, 1996.
[33] L.J. Farrugia, J. Appl. Cryst. 30 (1997) 565.
[34] C.F. Macrae, I.J. Bruno, J.A. Chisholm, P.R. Edgington, P. McCabe, E. Pidcock, L. Rodriguez-Monge, R. Taylor, M. Towler, J. van de Streek, P.A. Wood, J. Appl. Crystallogr. 39 (2008) 453–457.
[35] E.J. Moon, Y.M. Lee, K.W. Kim, Oncol. Rep. 10 (2003) 617–621.
[36] T. Mosmann, J. Immunol. Methods 65 (1983) 55–63.
[37] A. Bsndyopadhyay, Y. Zhu, S.N. Malik, J. Kreisberg, M.G. Brattain, E.A. Sprague, J. Luo, F. L'opez-Casillas, L.Z. Sun, Oncogene 21 (2002) 3541–3551.